

DISCREPANCY ANALYSIS BETWEEN CLOSE-RANGE PHOTOGRAMMETRY AND TERRESTRIAL LIDAR

Gustavo O. Maldonado^a, Sam R. Newsome^b, Marcel Maghiar^a,
Jerome T. Clendenen^a and N. Mike Jackson^a

^a*Department of Civil Engineering and Construction Management, Georgia Southern University,
Statesboro, GA 30460-8077, gmaldonado@georgiasouthern.edu,
<http://ceit.georgiasouthern.edu/cecm/>*

^b*Thomas and Hutton, 50 Park of Commerce Way, Savannah, GA 31405, USA,
info@thomasandhutton.com, <http://www.thomasandhutton.com>*

Keywords: 3D Structural Models, Close-Range Photogrammetry, LiDAR, Discrepancy Analysis.

Abstract. This work presents a comparison of spatial measurements performed on 3D virtual models of civil structures against actual field measurements completed on the related real objects. The virtual models were generated by two different techniques. In one instance, the 3D models were produced via close-range photogrammetry (CRP). Such models are based on numerous still-frame 2D photographs, post-processed with commercially available photogrammetric software. In the second approach, 3D point-cloud models were generated via terrestrial light detection and ranging (LiDAR), laser scanning. For comparison purposes, two case studies were conducted. The first involved a single story structure at the campus of Georgia Southern University. The second case was a multi-level Maya ruin at Dzibilchaltun, Merida, Mexico. For accuracy comparisons, various benchmarks were established around the structures following accurate closed-traverse procedures. The benchmarks served as standard georeferenced points. Several physical target points were then marked on the exterior walls of the structures. They are referred here as reference wall points (RWPs). The actual RWPs were then measured with typical laser-based total-station instruments. After photographs were taken and laser scanning of the structures were completed, the coordinates of the RWPs points were also determined from the respective virtual models. The virtual coordinates were then compared against the ones obtained with the total-station instruments. Coordinates and distances from each procedure were compared to determine discrepancies. Results of this study demonstrate that close-range photogrammetry can provide accurate enough information to be employed as an alternative 3D measuring and modeling technique for surveying and civil engineering applications involving structures and areas within the size range covered in the presented case studies. Additionally, several recommendations on the use of CRP and laser scanners are presented.

1 INTRODUCTION

1.1 Purpose of the study

This work involves the study of spatial discrepancies in measurements acquired from 3D virtual models of civil structures and related areas. The 3D models were generated by two modern approaches, CRP and laser scanning. The purpose of this work is to compare positions and distances from the virtual models against field measurements acquired by classical, laser-based, total-station, surveying instruments. That is, the total-station devices were employed as the control instruments. In the photogrammetric approach, the software-generated models were produced from sets of multiple 2D overlapping photographic images, taken from different locations around the structure to be modeled. This technique is now known as CRP and has substantially evolved in the last 30 years. Modern surveying scanning equipment was also employed to create 3D point-cloud models of the same objects using laser scanners. In the last years, constant improvements in computer processing times, photographic camera definitions and unmanned aerial vehicles (UAVs) capabilities have increased the use of CRP. It is now becoming a popular alternative for surveying tasks, especially in projects where the camera-to-object distances are relatively short.

Two case studies were selected for the mentioned comparison based on the location and size of structure. The first was located near the Recreation Activity Center (RAC) on the campus of Georgia Southern University, at Statesboro, Georgia, USA. This site contained several buildings of varying sizes, but a small brick storage building was chosen for its size and location. The second was located outside the city of Merida in Dzibilchaltun, Yucatan state of Mexico. The place is a national historical Maya site administered by the Mexican National Institute of Anthropology and History (INAH as per its Spanish acronym). The Temple of the Seven Dolls was selected as it was the most complete structure and one of the largest at the site.

Several other studies have focused on the accuracy of photogrammetry and laser scanning in past few years. While the studies are similar to this work, they present differences. This study placed actual targets, reference wall points (RWPs), on the structure being measured, which allowed the comparison points to be precisely located in the models. The other studies used features on the structures to locate their comparison points. The method in which the points were compared also differed. This research used two different approaches, while most others only used one. The first approach considers coordinate discrepancies to compare differences in the actual coordinate readings of point locations and was used by other studies. The second approach in this study employs distance discrepancies from a center point. In the latter method, distances are calculated from a random center to other surrounding points. The distances acquired from each virtual model are then compared to the distances acquired by a total-station instrument.

1.2 Brief History and Types of Photogrammetry

Photogrammetry is a land surveying technique that uses data extracted from two-dimensional photo images and aligns them into a three-dimensional model (Dai and Lu, 2010). The origins of photogrammetry can be traced back to Leonardo da Vinci's work with optical perceptivity in 1492. In his book, Sanjib Ghosh (2005) summarizes the main historical developments on photogrammetry. He indicates that in 1759 John Heinrich Lambert introduced the concept of inverse central perspective and space resection of conjugate images. This allowed to mathematically find, in space, the location where a picture was taken from.

Ghosh indicates that, in 1883, Guido Hauck established the relationship between projective geometry and photogrammetry. This relationship is considered the fundamental geometric concept and basis to which most classic analytical photogrammetric developments are based on. As has been the case in numerous fields, the availability of computational power catalyzed advancements and developments in photogrammetry.

Today, there are two main types of photogrammetry employed in civil engineering and surveying applications, close-range and aerial. Aerial Photogrammetry (AP) is more expensive since it requires relatively large aircrafts equipped with high-resolution, survey-grade cameras, to fly over the areas to be modeled. Close-Range Photogrammetry (CRP) is similar to AP as most of the same basic principles apply. The main difference between the two is the distance from the camera to the object. In CRP the object-to-camera distance is less than 1000 ft or 300 m (Matthews 2008). Additionally, CRP can be accomplished by employing consumer-grade cameras from the ground and/or mounted on the now available unmanned aerial vehicles (UAVs). CRP has not always been a preferred method. As indicated by Matthews, “...advances in commercially available and cost-effective three-dimensional measuring and modeling (3DMM) software, high-resolution digital cameras, and high-performance laptop computers have revolutionized the CRP process.”

Dai and Lu (2010) indicate that there are two major factors affecting the accuracy of a photogrammetric model. The first is a system error due to lens distortion and can now be easily corrected by software. The second are human errors mostly due to the imprecise marking of points in two different photos. This can be overcome by marking the points in three or more photos. As a consequence, most programs require the points to be marked in at least three photos.

1.3 Previous Studies

Research studies similar to this one have been performed in recent years. Some of them involve accuracy comparisons, while others focus on other aspects of photogrammetry and laser scanning. Dai et al. (2013) compares photogrammetry and laser scanning accuracy, quality, time efficiency, and cost. They produced models using photogrammetry and laser scanning and compared the spatial coordinates against those obtained by a total station. One notable difference between Dai's study and this research is the method of point comparison. Dai et al. used the corners of the infrastructure and other feature points on the surface for the comparison points, while this study uses physical targets placed on the structure. Dai's study employed a ground truth model that was created using the total station data. This was then used as the reference for the accuracy comparison by registering the point clouds produced by laser scanning and photogrammetry into same coordinate frame as the ground truth model. Three types of photogrammetry software were used by Dai, et al., in addition to the laser scanner. They conducted several case studies to obtain the necessary data, which were a concrete beam bridge, a stone building, and concrete arch bridge. The concrete beam bridge produced an average error of between 6.44 cm and 14.06 cm for the photogrammetry and 0.48 cm to 0.56 cm for the laser scanner. The stone building had similar results with an average error between 6.83 cm to 10.46 cm for the photogrammetry and 0.59 cm to 0.67 cm for the laser scanner. In their last case study, only the photogrammetry was compared against the ground truth model resulting in an average error between 6.52 cm and 9.48 cm. Dai et al. also made note of the point density that each model produced. The photogrammetry models had a point density between 3,200 and 10,000 points per square meter, while the laser scanner consistently had over 10,000 points per square meter. Dai et al. concluded that

photogrammetry and laser scanning produce dense point clouds that were satisfactory for visualization and photogrammetry offered a good alternative to laser scanning when accuracies required were greater than 8 cm.

Other study on the accuracy of CRP by Yakar et al. (2010) shows volume calculation comparisons between CRP and a robotic total station. However, they used the robotic instrument in a manner similar to a laser scanner. The robotic total station was set to scan a sand pile at a spacing of 20 cm to produce a point cloud. They performed two additional scans with the robotic total station, one was at a 40 cm interval and the other was at a 100 cm interval. All three models from the robotic total station and the photogrammetry model were compared to the known volume that was obtained using a lorry. The photogrammetry model had a 93.63 percent accuracy, while the 20 cm total station model had a 96.35 percent accuracy. The two other total station models had slightly lower accuracies, but both were still above 90 percent. After the base line was established, Yakar et al. had a known volume of the material removed from the pile. They recreated the models and compared volume results to the known volume left in the pile. The results obtained by Yakar et al. were a 96.35 percent accuracy for the total station model, 63.13 percent accuracy for the photogrammetry model, and 89.04 percent accuracy for the geodetic method. They concluded that photogrammetry was a viable solution since it had significant time and cost savings.

A study by Sužiedelytė-Visockienė et al. (2015) focused on the accuracy of CRP for use in deformation of architectural structures. The purpose of that work was to explore if CRP had the required accuracy to catalog the current state of architectural pieces and track its deformation over time. The authors used standard photogrammetry software and high end consumer grade digital cameras for their work. The produced models were referenced to established control points for the comparison and reported an accuracy of 1 to 5 μm on two different ornaments inside a heritage architectural site. They concluded that photogrammetry could be used for documentation and geometric deformation monitoring of cultural heritage sites.

Gussenmeyer et al. (2008) compared different technologies and their methods. In this study, they used a laser scanner, a total station, and photogrammetry software to capture points on a historic castle. They did not perform a direct accuracy comparison, but focused on the quality of the models produced and on the quality of the points acquired. This was accomplished by using the points collected by each system to produce a wireframe that was composed of 21 windows. A quote from Gussenmeyer et al. explains why this method was used, *“For comparing laser and surveying data, a point to point comparison makes no sense, since laser scanning technique does not allow choosing the point to be measured.”* By using this approach, they found that 88 percent of the points fell in a range of -2 cm to 4 cm when comparing differences in the photogrammetry and laser scanner meshes. They concluded that each system had its own limitations and strengths depending on what the site situations demanded, thus one system could not be recommended over the others.

2 METHODOLOGY

The equipment and data acquisition processes, employed by this study, are described in the following two subsections.

2.1 Equipment

The photogrammetry component of this work included three cameras, a standard desktop

computer, a photogrammetric processing software and an unmanned aerial vehicle. On the other hand, laser measurements included a scanner and two total-station instruments. The laser scanner required targets, proprietary software, and various tripods. The total station also required additional items such as prisms and tripods.

The three cameras used in this project were a Nikon D800, Canon EOS 5D Mark III, and GoPro Hero 3 Plus, Black Edition. The Nikon D800 is a single-lens reflex digital still frame camera with 36.3 effective megapixels. It was equipped with a fixed wide-angle Nikkor 28mm autofocus lens for the duration of the project. The Canon EOS 5D Mark III is a digital single-lens reflex still camera with 22.3 effective megapixels. It employed a fixed wide-angle Ultrasonic 20mm autofocus lens for the first seven weeks of the study. After that, the Canon was refitted with a fixed wide-angle Ultrasonic 24mm autofocus lens with image stabilization. The lens change was necessary to allow the Canon to be mounted in an unmanned aerial vehicle's gimbal assembly for CRP. The GoPro Hero 3 Plus, Black Edition, is a digital video camera with 12 effective megapixels. It was originally equipped with a fish-eye lens from the factory. This lens was replaced with a flat wide-angle lens with less distortion to allow the GoPro to be more compatible with the photogrammetry software. This is no longer necessary as most software now has built-in correction for the GoPro's fish-eye lens.

An important component of this study is the CRP software used for 3D model generation, Agisoft's PhotoScan Pro. It is a 3D modeling, measuring, and geo-referencing software. Three different versions of PhotoScan Pro were used to produce models for this study, which are: version 1.1.0 build 2004, version 1.1.4 build 2021, and version 1.1.6 build 2038. PhotoScan uses photogrammetric triangulation and includes additional capabilities such as dense point cloud editing, classification, digital elevation modeling, and geo-referencing.

The equipment employed for laser scanning has three components. The main part of the system is the actual laser scanner, Leica Geosystems' ScanStation C10. It is a ground-based scanner capable of collecting 50,000 points per second at a maximum range of 300 meter. According to Leica Geosystems the accuracy of this scanner is 6 mm for position, 4 mm for distance, and 12 seconds for horizontal and vertical angles. The next required piece of equipment are scanner registration targets, used to stitch the different scans together into a common system of reference. There are different types of registration targets that can be used with the C10 instrument. Three of them were employed in this study, the HDS twin target pole system, the 6" blue tilt and turn targets, and 6" spheres. The last needed component to operate the mentioned scanner is the Leica Cyclone software package. It presents many capabilities, including point cloud registration, model creation, virtual surveying, and publishing. In this study, the main features used from Cyclone were the point cloud registration, measuring tools, and model creation. Some miscellaneous equipment used included a tripod for the scanner, target poles, and target tripods.

The total stations used for comparison were two Topcon model GPT-3200NW. This total station has an angular accuracy of 7 seconds with a minimum reading of 5 seconds in the horizontal and 10 seconds in the vertical. This instrument also has a single axis tilt compensator with a correction range of ± 3 minutes. Some miscellaneous equipment used included a tripod for the total station, prisms, prism poles, and prism pole tripods.

2.2 Data Analysis

The points used for comparison purposes consisted of RWPs that were applied to the actual physical structures in random locations. They were photographed, laser scanned and also measured with total-station instruments. Usually, several (about 10) RWPs were selected at

random from each side of a building (for a total of about 40). Two different approaches were used to compare the virtual measurements obtained from the 3D models to those acquired in the field with the total-station instruments.

The first comparison was done via the *Coordinate Discrepancy* approach where the easting (X), northing (Y), and elevation (Z) coordinates of the RWPs, obtained by the total-station instruments, were individually subtracted from the easting, northing, and elevation readings of the respective points in the 3D models. The second approach was *Distance Discrepancy*. In this scheme, a center point (one of the RWPs) is chosen on each side of the building, not necessarily at the center of each side, and several distances are calculated from those center points to other points (other RWPs). These distances are then compared (total-station distances subtracted from model distances) and the discrepancies presented in scatter plots.

3 CASE STUDY 1 – SMALL STORAGE BUILDING

The first case study consisted of a relatively small brick storage building, with a metallic roof, located near the Recreation Activity Center (RAC), on the Campus of Georgia Southern University. Figure 1 shows two pictures of the selected storage building.

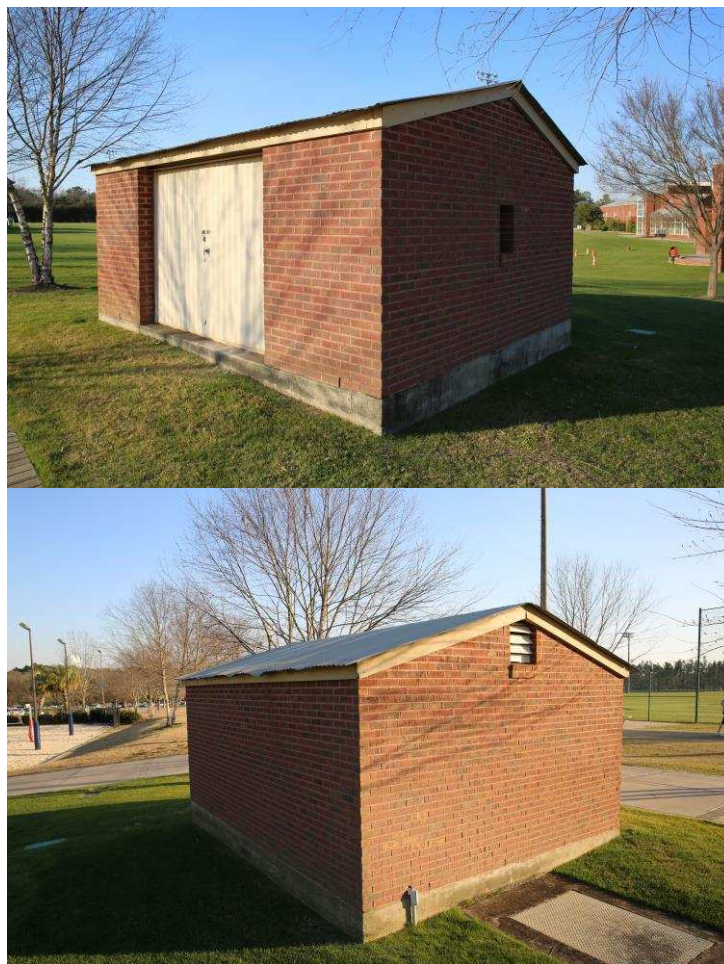


Figure 1: Pictures of Selected Small Storage Building at Georgia Southern University Campus

This location and structure was chosen as it had relatively little tree cover and no bushes near the building. Trees and bushes produce distortions or unwanted shades and empty areas (holes) in the models, especially in the photogrammetry one. The small size of the building

was another characteristic that led to this structure selection. The smaller size allowed multiple trials to be run within the limited time that undergraduate and graduate students have during a regular academic term (4 months).

Since the location of the building prevented the use of known benchmarks on campus, a closed traverse was completed to establish four benchmarks around it. For identification purposes, RWPs (stickers) were attached to the structure. They were marked with numbers on the four exterior walls.

Figure 2 shows views of the attained final 3D point-cloud model of the selected structure. Similarly, Figure 3 shows two views of the final 3D CRP model of the same structure.

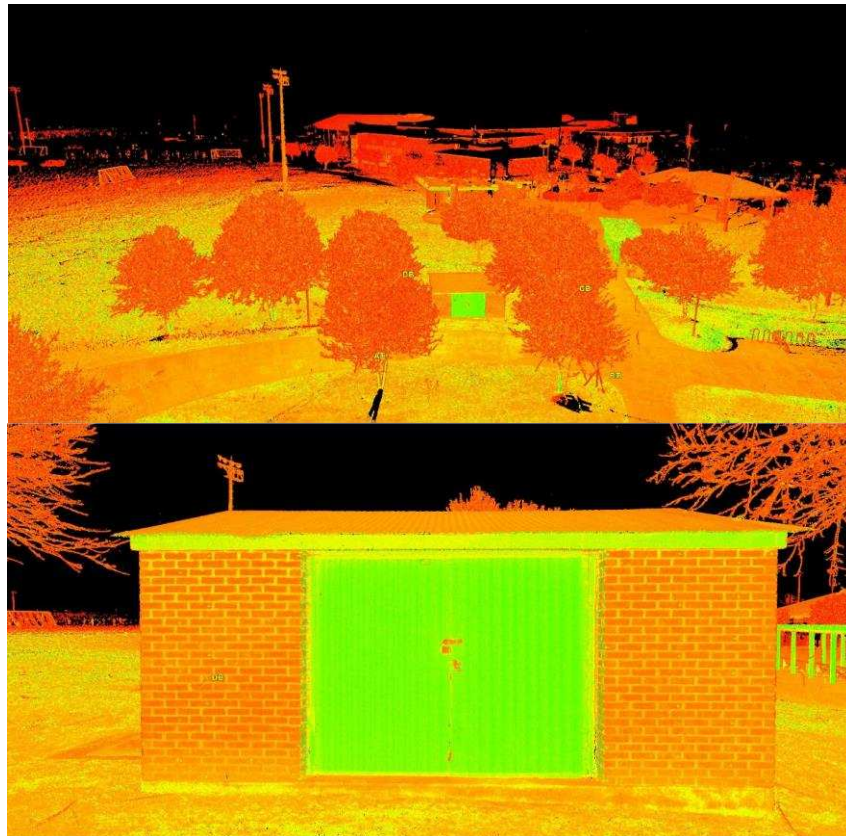


Figure 2: Far (top) and Front View (bottom) of 3D Point-Cloud Model of Selected Storage Building



Figure 3: Front (left) and Side View (right) of 3D CRP Model of Selected Storage Building

3.1 Surveying Control, Instruments, Data Collection and Processing

To compare the resulting 3D models, a control system was established around the selected storage building. As indicated in Figure 4, four benchmarks were materialized with 12-inch long, steel nails around the building and a closed traverse was performed and locally referenced. The benchmarks were established with high accuracy as this would serve as the control for this case study. The internal and external angles of the closed traverse were measured by the approach known as closing-the-horizon, employing the direct and reverse modes of the instrument. After local corrections at each vertex, the final angular error of closure was 21 seconds. Distances were measured with the total-station instruments and the final longitudinal error of closure, in the traverse, was 0.003 ft, which corresponded to an approximate longitudinal precision of 1 (one) unit in 59,000 units.

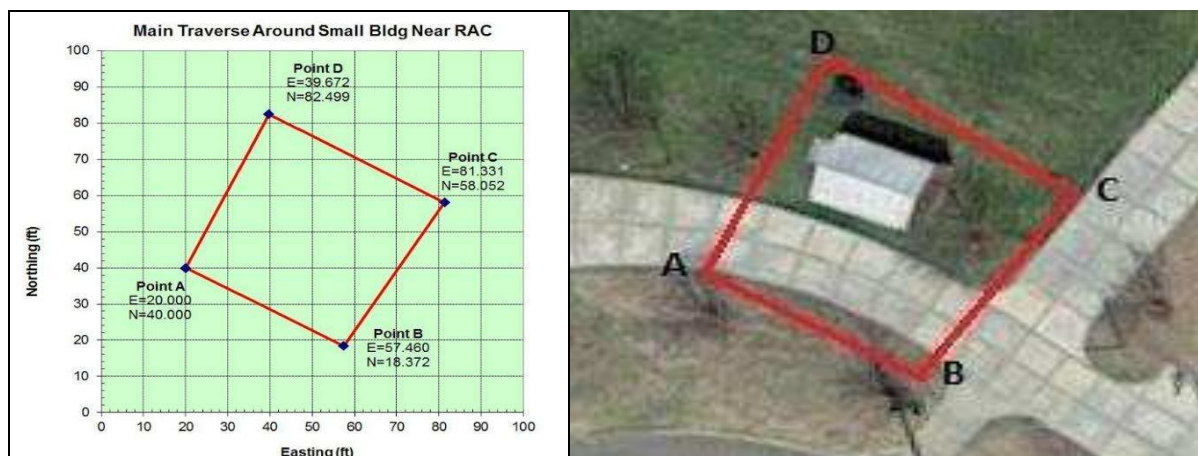


Figure 4: Closed Traverse around the Selected Storage Building. Easting and Northing Relative Coordinates of Four Benchmark Vertices (left). Google Map Plan View (right) of Selected Structure

To complete the coordinates of the reference benchmarks, the relative elevations of points A, B, C, and D were determined using a modern auto-level instrument. Since point C is the lowest point of the four, it was selected to be at a reference elevation of 10 ft. The elevations of the remaining points were then computed from this arbitrary datum. The adopted final elevations were the average of two complete closed loops. The total-station instrument was employed as the control instrument that all other measurements would be compared to. The purpose was to compare a trusted standard instrument to the newer available technology. When collecting the points from the building, the total station occupied one of the control benchmarks. The northing, easting, and elevation coordinates of the point would be entered into the instrument along with the known azimuth to another point. This would set the instrument to the reference coordinate system and give the instrument the direction of north. The operator would then aim the instrument at points on the building (RWPs) and obtain their coordinates using reflectorless mode. The operator would continue collecting points until the instrument need to be moved and the set up process repeated for a new point.

The photogrammetry model was produced next. As stated earlier, the photogrammetry software selected for this accuracy comparison was Agisoft's PhotoScan Professional Edition, version 1.1.6. Several other options were evaluated, but PhotoScan was selected as it had the required features for the scope of this study. Four different models were produced of the RAC storage building, one from each of the three cameras and a combined photo set from the Cannon and Nikon cameras. The Cannon 5D Mark III camera model was selected as it

produced the clearest model of the structure. The RAC storage building model used for the comparison was created using 118 pictures. The photo set consisted of 60 pictures from ground level and 58 pictures from a ladder placed close to the building near the center of each of the four sides. The camera was set at the highest megapixel setting of 22.3 with JPEG selected as the file compression format. The camera-to-object distances for this case study ranged from 5 to less than 20 ft. When preparing PhotoScan to process the pictures, the default settings were used for each process. The standard processes used were “align photos,” “build dense cloud,” “build mesh,” and “build texture.” The standard settings for the align photos operation were accuracy set to high with pair preselection disable under the general options. Under the advanced options the key point limit was set to 40,000 and tie point limit to 1,000 with constrain features by mask disabled. The following default settings were used for the build dense cloud operation, quality set to medium, depth filtering to aggressive, and reuse depth maps disabled. Under the general tab of the build mesh operation the settings were arbitrary surface type, dense cloud source data, medium face count and 200,000 custom face count. The advanced tab had two additional setting for interpolation and point classes, both were left at the default setting of enable and all respectively. The final operation was build texture. In the general settings of build texture, mapping mode was set to generic, texture from was set to all cameras, blending mode to mosaic, texture size to 4096 and texture count to 1. Under the advance tap, there was only one setting, color correction was set to no.

The processed model is shown in Figure 3. After the model was created using PhotoScan, it was geo-referenced to the relative coordinate system that was used by the total station. The geo-referencing is necessary since the photogrammetry software creates its own relative coordinate system when the models are generated. Without relating one coordinate system to the other, it would be impossible to compare the coordinates of the points across multiple technologies. The photogrammetry model was georeferenced by selecting, on the walls of the structure, four of the RFPs that were measured with the total station. The selected points were then marked in PhotoScan by placing markers in three or more photos containing each point. The purpose of marking the points in multiple photos is to allow the software to triangulate the locations of the points using the camera locations that have already been processed. After the points were marked in PhotoScan, the coordinates of the points from total station were entered. This method of geo-referencing was necessary as the control benchmarks were cut from the model by the photogrammetry program. It would have been preferable to use the control benchmarks. This is because the employed method can introduce error from the work attained by the total station instruments. By doing this, the researchers assumed all the points collected by the total station are accurate, which may not always be the case. After the model was geo-referenced, the coordinates of the other points were collected by placing markers on the model at the location of the selected points. After all the markers were placed, the view estimated command in PhotoScan was used to calculate the coordinates of the marked points. Figure 3 shows a marked and referenced model.

The laser scanner used for this project was the Leica Geosystems ScanStation C10. The scanner registration targets employed were the Leica HDS twin target pole system and the Leica 6” blue tilt and turn target. A total of six targets were used when the scanning was performed. The Leica HDS twin target poles were placed on the four benchmarks and two Leica 6” blue tilt and turn targets were placed in various locations depending on the scanner location. A total of four scans were performed with the scanner placed at each corner of the building at approximately a 6 ft distance from the structure. This allowed the scanner to collect two sides of the building and at least three targets. The scanner was set to high resolution to ensure enough point density was achieved for point collection. This was the only

time a complete project was done using high resolution scans. The high resolution scans are not needed in most situations. This is because superposed multiple medium resolution scans will increase the density of the resulting point cloud. Also high resolution scans require additional time over medium resolution scans. A high resolution normally takes about twenty-seven minutes to complete, while a medium resolution only takes six minutes to complete. The high resolution scans were used in this case because of the corner location selected for the scanner, with smaller angle of incidence as wall segments were scanned farther from the scanner station. Since the building was small, the scanner was placed at the corners which allowed the operators to reduce the number of scans required for this building. If each face of the building were scanned individually, it would have required a minimum of eight scans and additional scanner registration target locations as it would have been more difficult to see three common targets in each scan. The four high resolution scans were registered using Leica Geosystems' Cyclone software. The registration process combines the scans together using the scanner registration targets that are in each scan. Registration requires a minimum of three common targets between two scans to be stitched together. The software continues stitching neighboring scans together until all the scans are combined. After all the scans are registered together, the resulting model was georeferenced to the total station coordinate system. Georeferencing in Cyclone is accomplished by importing a comma delimited text file containing the coordinates of the benchmarks. Cyclone uses the information in the text file to create a control scanworld. The control scanworld is then registered with the previous complete registration which geo-references the model to the correct coordinate frame. As with any process there is always some error involved. The errors in the registration for this model, after and before geo-referencing were 0.013 ft (0.156 in.) and 0.007 ft (0.084 in.), respectively. With the model georeferenced, the coordinates of the comparison points were collected from the virtual model. This was accomplished by selecting a point in the model that was as close as possible to the center of one of the RWPs. Figure 5 Shows one of those RFP points at one wall of the structure after been scanned. The coordinates were recorded at that point and this was repeated until all RWPs were collected.



Figure 5: Point Marking Example. RPF (Reference Wall Point) at One Brick Wall of Storage Building.

3.2 Results from Case 1

To determine discrepancies in the measurements, ten points on each wall (RWPs) were selected from the originally attached 299 RWPs. The results are presented in the following tables and figures. Table 1 contains a summary of the results from the Coordinate Discrepancy approach for both, the laser-scanned and photogrammetry models versus the field coordinates obtained via total-station instruments. That table includes the maximum discrepancies, minimum discrepancies, mean values, root mean square (RMS) values and standard deviations. Each of Figures 6, 7, 8 and 9 shows a graph of distance discrepancies measured from one of the four center points. Similarly, Tables 2, 3, 4 and 5 present statistical summaries for the respective distance discrepancies from each of the four center points. Each figure/graph discusses the results from a single center point that was selected from side A, B, C, or D, corresponding to the south-, east-, north- and west-facing walls. In these figures, distances from comparison points, to a selected center point, were determined by Equation 1. During data processing, it was evident that coordinates of a few points were erroneously collected by some of the multiple student operators. Those points were removed from the analyses. They are indicated as outliers in the respective tables and figures.

$$D_i = \sqrt{(x_i - x_c)^2 + (y_i - y_c)^2 + (z_i - z_c)^2} \quad (1)$$

$x_i, y_i, \& z_i = \text{coordinates of comparison point}$
 $x_c, y_c, \& z_c = \text{coordinates of center point}$

Item	Laser Scanner - Total Station			Photogrammetry - Total Station		
	X	Y	Z	X	Y	Z
Maximum Value (ft)	0.0810	0.0480	0.5750	0.0876	0.0470	0.6015
Minimum Value (ft)	0.0000	0.0000	0.0000	0.0002	0.0004	0.0009
Mean Value (ft)	0.0097	0.0090	0.0741	0.0169	0.0103	0.0913
RMS Value (ft)	0.0188	0.0140	0.2003	0.0223	0.0144	0.2095
Standard Deviation (ft)	0.0163	0.0109	0.1885	0.0147	0.0102	0.1910
Outliers Removed	A047, C006			C039		

Table 1: Coordinate Discrepancy Statistical Data for Storage Building with Outliers Removed

Item	Laser Scanner - Total Station	Photogrammetry - Total Station
Maximum Value (ft)	0.2293	0.2063
Minimum Value (ft)	0.0003	0.0010
Mean Value (ft)	0.0389	0.0455
RMS Value (ft)	0.0756	0.0697
Standard Deviation (ft)	0.0666	0.0556
Outliers Removed	A047, C006	C039

Table 2: Statistical Data for Discrepancies in Distances Measured from Center Point A066, with Outliers Removed, at Storage Building

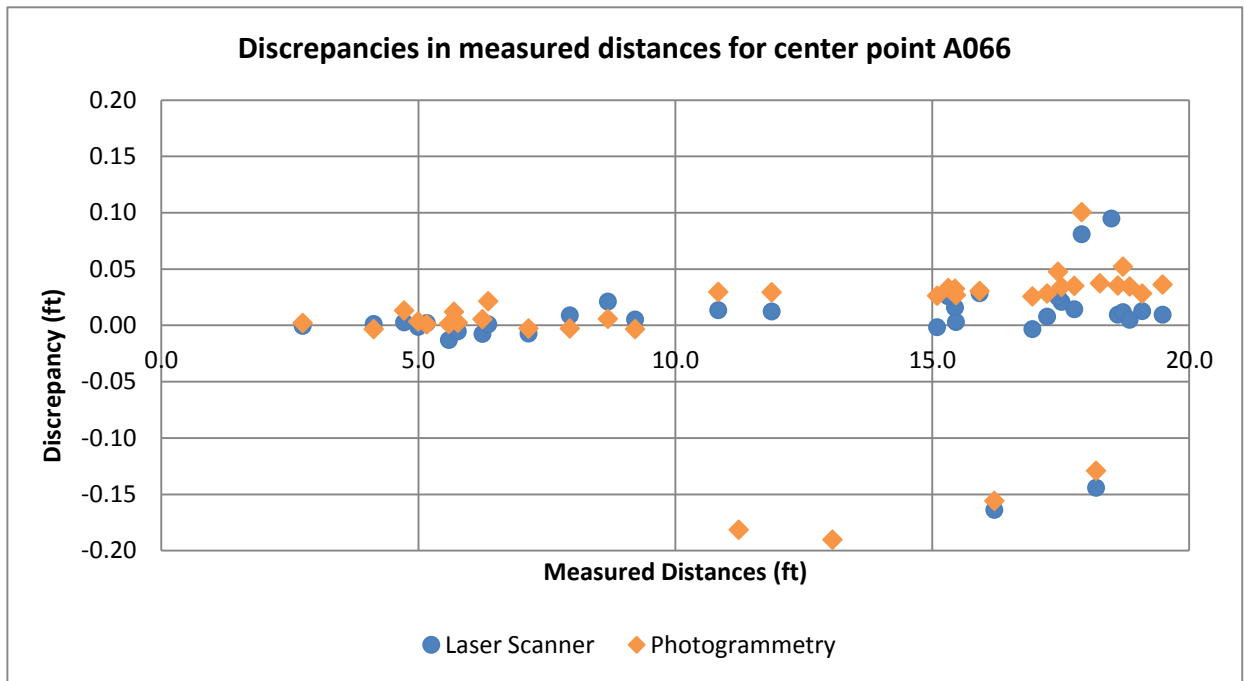


Figure 6: Discrepancies in Measured Distances from Center Point A006, at Storage Building

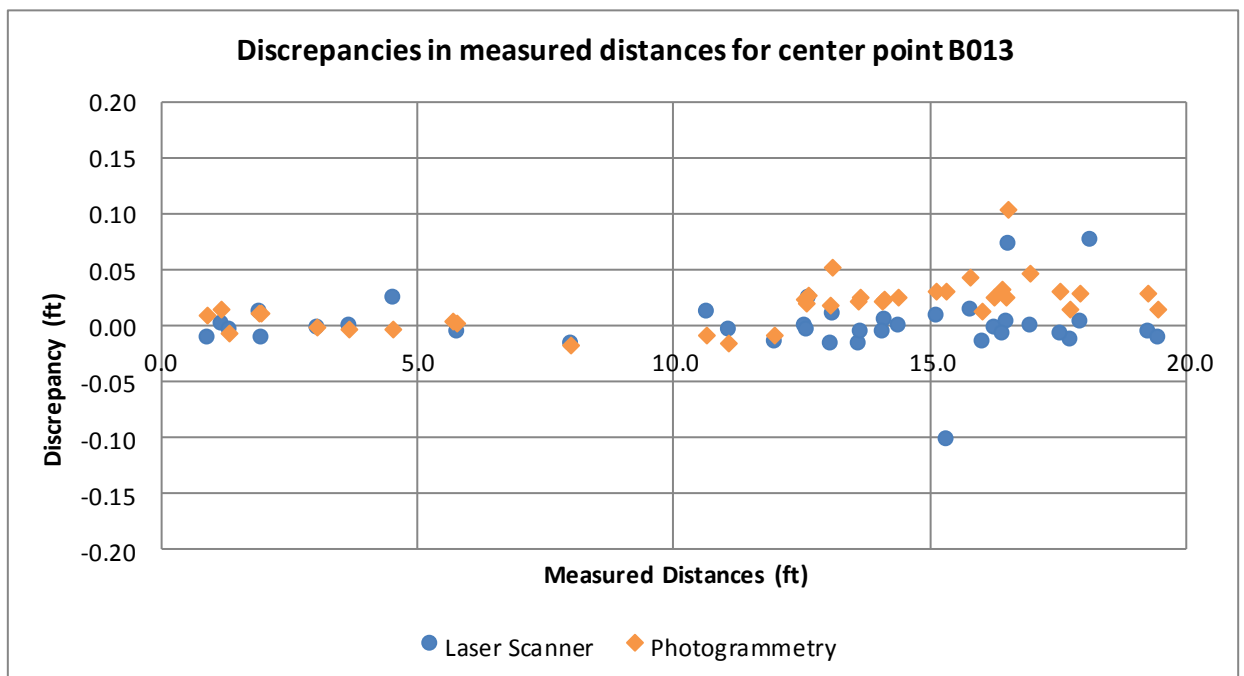


Figure 7: Discrepancies in Measured Distances from Center Point B013, at Storage Building

Item	Laser Scanner -Total Station	Photogrammetry - Total Station
Maximum Value (ft)	0.0776	0.1044
Minimum Value (ft)	0.0001	0.0016
Mean Value (ft)	0.0119	0.0230
RMS Value (ft)	0.0202	0.0286
Standard Deviation (ft)	0.0169	0.0186
Outliers Removed	A047, C006	C039

Table 3: Statistical Data for Discrepancies in Distances Measured from Center Point B013, with Outliers Removed, at Storage Building

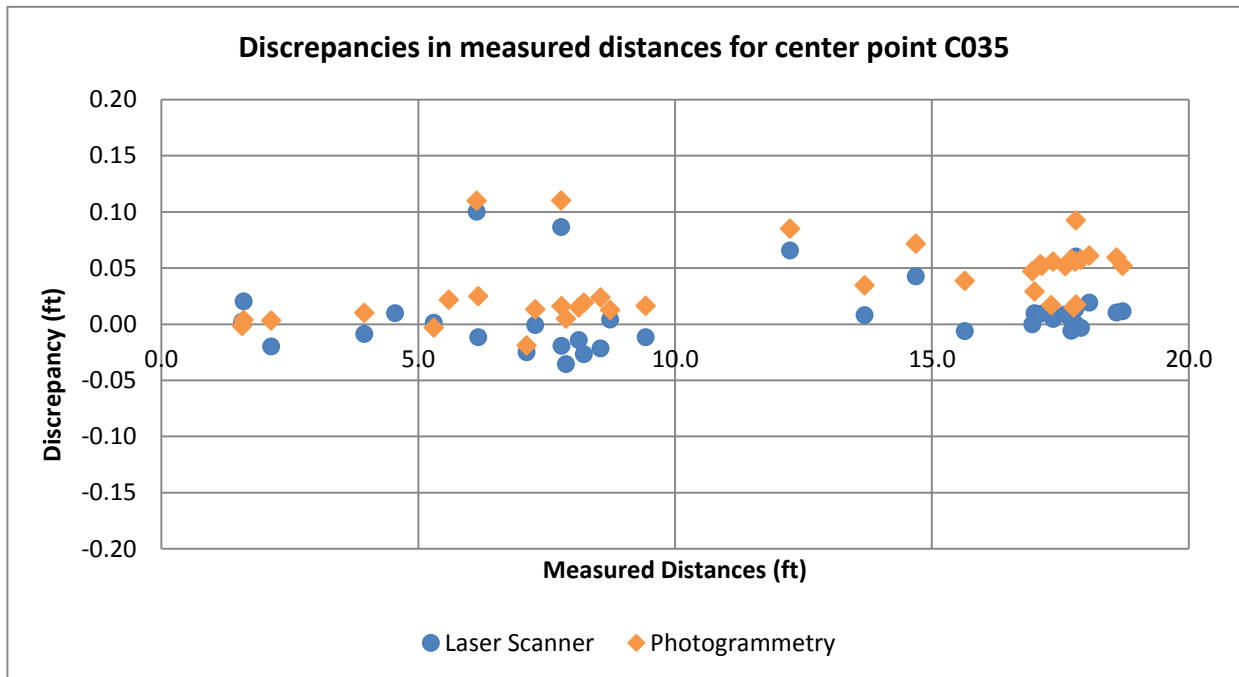


Figure 8: Discrepancies in Measured Distances from Center Point C035, at Storage Building

Item	Laser Scanner -Total Station	Photogrammetry - Total Station
Maximum Value (ft)	0.1000	0.1102
Minimum Value (ft)	0.0001	0.0015
Mean Value (ft)	0.0191	0.0389
RMS Value (ft)	0.0300	0.0467
Standard Deviation (ft)	0.0238	0.0297
Outliers Removed	A047, C006	C039

Table 4: Statistical Data for Discrepancies in Distances Measured from Center Point C035, with Outliers Removed, at Storage Building

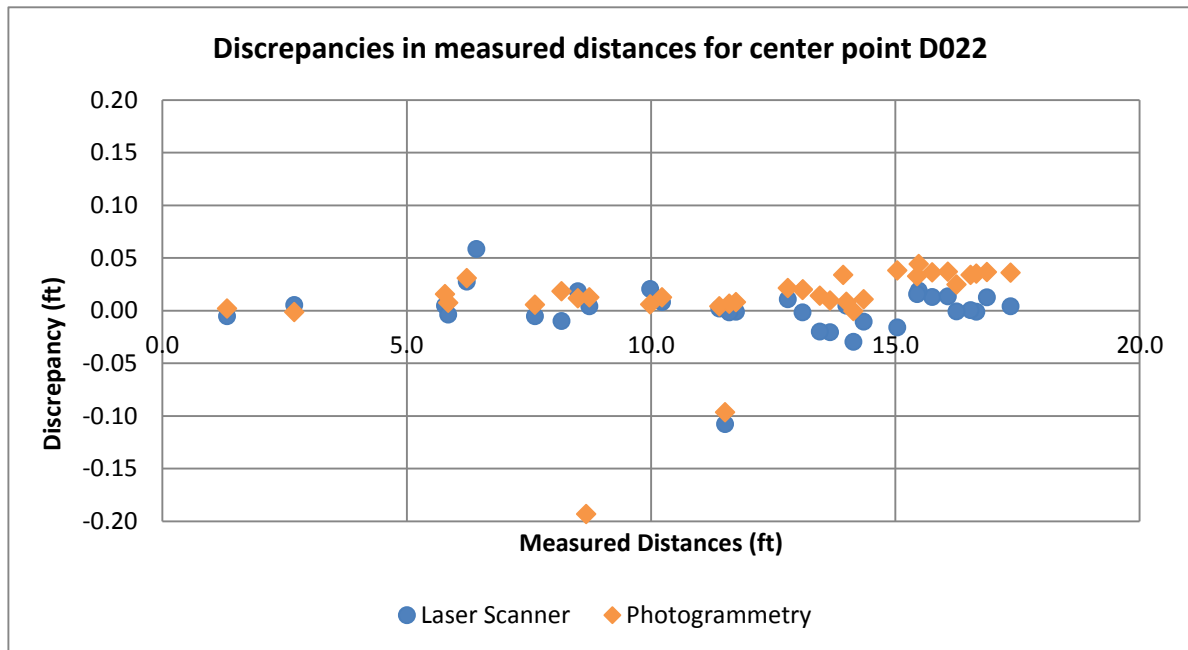


Figure 9: Discrepancies in Measured Distances from Center Point D022, at Storage Building

Item	Laser Scanner - Total Station	Photogrammetry - Total Station
Maximum Value (ft)	0.5570	0.5804
Minimum Value (ft)	0.0006	0.0004
Mean Value (ft)	0.0522	0.0610
RMS Value (ft)	0.1297	0.1316
Standard Deviation (ft)	0.1218	0.1214
Outliers Removed	A047, C006	C039

Table 5: Statistical Data for Discrepancies in Distances Measured from Center Point D022, with Outliers Removed, at Storage Building

4 CASE STUDY 2 – MAYAN RUIN

The structure selected for this case is a Mayan ruin, the Temple of the Seven Dolls. It is located at Dzibilchaltun, outside the town of Merida in the Yucatan state of Mexico. The location is a national historical Maya site administered by the Mexican National Institute of Anthropology and History (INAH as per its Spanish acronym). This project was a partnership between Georgia Southern University, Universidad Anáhuac Mayab, and INAH. This temple was selected due to the preservation work INAH is conducting for this structure and the opportune visit of several Georgia Southern students for study abroad in Mexico at Universidad Anáhuac Mayab. Additionally, this structure is much larger than the one considered in case 1. An added bonus to this building was that INAH had already done substantial underbrush and tree removal around the temple. This was the largest structure

modeled for this study. The temple consists of a three tiered structure with small ruins around it. The bottom section presents a large pyramidal shaped base with stairs leading up to the second section consisting of a square structure with four windows, four doors, and an inner chamber. This chamber protruded through the roof of the second tier forming the third, which was also square, but significantly smaller with just one exit to the roof on the southern side. Similar to the study in Case 1, there were no known benchmarks located near the structure. Therefore, a closed traverse was completed to establish four benchmarks around it. Forty (40) WRPs were marked on the walls of this structure. These WRPs were marked by blue painter's tape with a black crosshair in their center. Later, it was realized this was not a good choice of colors because it was difficult to visualize in the collected point clouds. Figure 10 shows the two different 3D models obtained for this structure.



Figure 10: 3D Point-Cloud Model (top) and 3D CRP Model (bottom) of the Temple of the Seven Dolls

4.1 Surveying Control, Instruments, Data Collection and Processing

Four control benchmarks were established with steel stakes around the temple and a four-vertex closed traverse was performed. They were labeled A, B, C, and D and their approximate relative location with respect to the temple is shown in Figure 11. The position of bench mark A was assumed to be 600 ft in the X direction (easting) and 300 ft in the Y direction (northing). The initial azimuth from point A to B was approximately measured with a hand compass. Therefore, the geographic orientation of the traverse is just approximate, within $\pm 5^\circ$.

After local corrections at each vertex, the final angular error of closure was 5 sec. Distances were measured electronically and the longitudinal error of closure in the traverse was 0.0226 ft, which corresponded to an approximate longitudinal precision of 1 (one) unit in 25,184 units. To complete the coordinates of the reference benchmarks, the relative elevations of points A, B, C, and D were determined using a modern auto-level instrument. Since point A was the starting point, it was selected to be at a reference elevation of 32.808 ft or 10 m. The elevations of the remaining points were then computed from this arbitrary datum. The total-station instruments were employed to establish the control benchmarks and to collect in the field coordinate measures of RWPs in reflectorless mode.

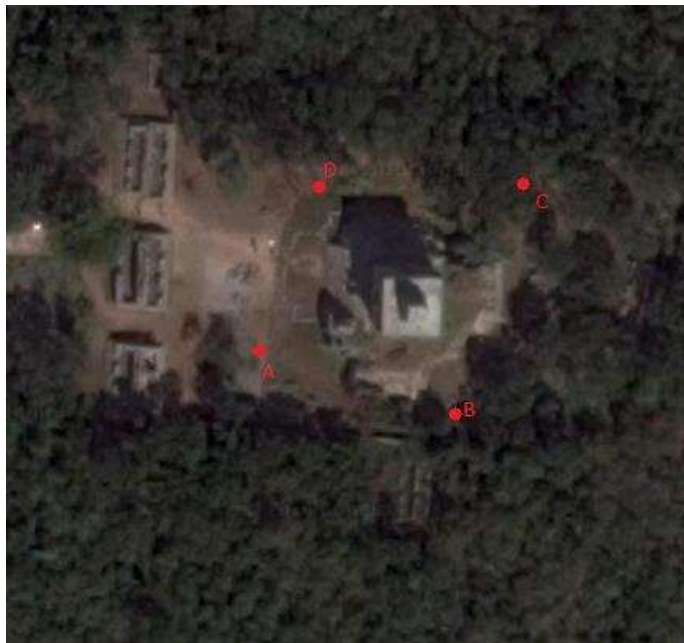


Figure 11: Google Map Plan View Showing the Approximate Relative Location of the Temple and the Employed four Benchmarks

The photogrammetry model was produced via the Agisoft's PhotoScan software package, Professional Edition, version 1.1.6. Unlike Case Study 1, this time only one model was produced. This was in part due to the number of photos needed to model such a large structure in great detail. The cameras used to produce the model were the Nikon D800 and the GoPro Hero 3 Black Edition. The Nikon was used to collect photos of the first and second tiers of the structure from the ground. The GoPro was attached to a custom built quadcopter and used to obtain downward vertical photos and pictures of the third tier. The temple model used for comparison was created using a total of 2433 pictures. The photo set consisted of 1166 pictures for the Nikon on the ground and 1267 pictures from the GoPro in the air. Both

cameras were set to their maximum resolutions, which were 36.3 megapixels for the Nikon and 12 megapixels for the GoPro. The camera to object distances for this case were 75 ft or less, since the wide angle lenses used required greater distance to capture large sections of the temple.

In this case study, the standard PhotoScan settings were not adequate to process the pictures. Typical processes such as “align photos,” “build dense cloud,” “build mesh,” and “build texture” were used, but they required the default setting to be modified before a successful model was produced.

In the align photos process, the key point limit was set to zero and the tie point limit was set 100,000. Setting the key point limit to zero allowed the software to target the maximum number of feature points in each photo. Increasing the tie point limit from 1,000 to 100,000 maximized the number of possible matches between photos. These two modifications reduced the possibility of photo alignment problems showing up in the later processing steps. This was necessary due to the distance that the photos were taken from.

Under the build dense cloud settings, the quality was set to medium and the depth filtering was set to mild. The first test models produced were done with the quality set to lowest, which allowed for shorter processing time. The final model used for the comparison was done at medium quality and required thirty-four days to process. The processing time was partly dependent on the computer hardware used. For this study, the computer selected was a Lenovo ThinkCentre with an Intel i7 3.40 GHz CPU and 32 gigabytes of memory. The depth filtering was set to mild instead of aggressive as some of the test models had a severe lack of detail. Once the depth filtering was set to mild it eliminated the problems with parts of the structure losing detail. The depth filtering setting controls how many small details are included in the models.

The settings for the build mesh were only modified on the face count. The face count controls the maximum number of polygons in the final mesh and was set to high in this model. This was done to help with creation of the model and to help sharpen the lines of the model. In the final processing step, build texture, the default settings were used. The final step just applies texture to the mesh and thus has little effect on the actual model. If a texture problem is found, the settings can be adjusted to correct it, but expect an extremely long processing time.

The final photogrammetry model can be seen in Figure 10 (bottom). After the model was created using PhotoScan, it had to be georeferenced to the relative coordinate system that was used by the total station. The geo-referencing is necessary since the photogrammetry software creates its own relative coordinate system when the models are generated. Without relating one coordinate system to the other, it would not have been possible to compare the coordinates of the points across multiple technologies. The photogrammetry model was georeferenced by selecting four of the RWPs that were measured with the total station. The selected points were then marked in PhotoScan by placing markers in roughly 20 photos containing each point. The four points selected from the model for geo-referencing were N8, S2, E4, and W8. After the points were marked in PhotoScan, the coordinates of the points obtained via a total station were entered. This method of geo-referencing was necessary as the control benchmarks were cut from the model by the photogrammetry program. It would have been preferable to use the control benchmarks as this method can introduce errors from the measurements produced by the total station instruments.

After the model was georeference, the coordinates of the other points were collected by again marking the points in 20 photos. This marking of the comparison points was necessary because the RWPs were not visible on the finished model, unlike the Case 1 model. The loss

of the RWPs is due to two causes: (i) the distance that the photos were taken from and (ii) the type and color of RWPs markers used on the building. The blue tape used for the RWPs had low reflectivity, which led to the tape disappearing in both the photogrammetry and laser scanner models. After all the markers were placed on the RWPs points, the “view estimated” command in PhotoScan was used to calculate the coordinates of the marked points.

The laser scanner used for this project was the Leica Geosystems ScanStation C10. The scanner registration targets employed were Leica HDS twin target pole systems and Leica 6” blue tilt and turn targets. The Leica 6” blue tilt and turn targets were placed at the benchmarks, but since there were only three available targets they had to be moved between the four benchmarks. A total of ten Leica HDS twin target pole systems were used during the scanning of the temple. These targets were moved to multiple locations around the temple as the scanning progressed. There was a total of 17 target locations used around the temple; three on the north side, two on the south side, three on the east side, five on the west side and the four on the benchmarks. The size and particular geometric shape of the structure required a relatively large number of scans, 63, and numerous target locations.

Unlike the Case 1 study, the scanner was set to medium resolution. This was acceptable in this case due to the amount of overlap from scan to scan. Medium resolution was also preferred due to shorter scan time of six minutes versus twenty-seven minutes for a high resolution. The 63 medium resolution scans were registered using Leica Geosystems’ Cyclone software as previously explained. As with any process, there is always some error involved. The error in the registration for this model after geo-referencing was 0.01 ft or 0.12 in. With the model georeferenced, the coordinates of the comparison points were collected from the model. This was accomplished by locating the desired RWP on the model and picking a single point in the center of the cross-shaped mark. At times, this was difficult due to the blue tape and black cross used on the RWPs. This made it difficult to locate the exact center of the RWP and could have led to a lower accuracy for the laser scanner in this case study. The final 3D point-cloud model of the Temple is displayed in Figure 10 (top).

4.2 Results from Case 2

The coordinates of 40 RWPs were considered in this case study. The north side included 8 points and the east side 12. The other two sides included 10 points each. As it was done in Case 1, discrepancies were determined by using two different approaches, *Coordinate Discrepancy* of isolated points and *Distance Discrepancy* between chosen central points and other RWPs. In both approaches discrepancies were calculated by subtracting the total station measurements from the coordinates associated to either the laser scanner or photogrammetry virtual models.

Item	Laser Scanner - Total Station			Photogrammetry - Total Station		
	X	Y	Z	X	Y	Z
Maximum Value (ft)	0.1510	0.0812	0.5697	0.1208	0.0885	0.4964
Minimum Value (ft)	0.0029	0.0083	0.0027	0.0000	0.0000	0.0000
Mean Value (ft)	0.0521	0.0301	0.0289	0.0400	0.0282	0.0230
RMS Value (ft)	0.0756	0.0367	0.0899	0.0540	0.0394	0.0780
Standard Deviation (ft)	0.0520	0.0216	0.0865	0.0352	0.0267	0.0756
Outliers Removed	N7, W2			S7, W2		

Table 6: Coordinate Discrepancy Statistical Data for Mayan Temple, with Outliers Removed

Table 6 shows a statistical summary of the coordinate discrepancies of all 40 points, with outliers removed. They are presented in Tables 7, 8, 9 and 10 and Figures 12, 13, 14 and 15.

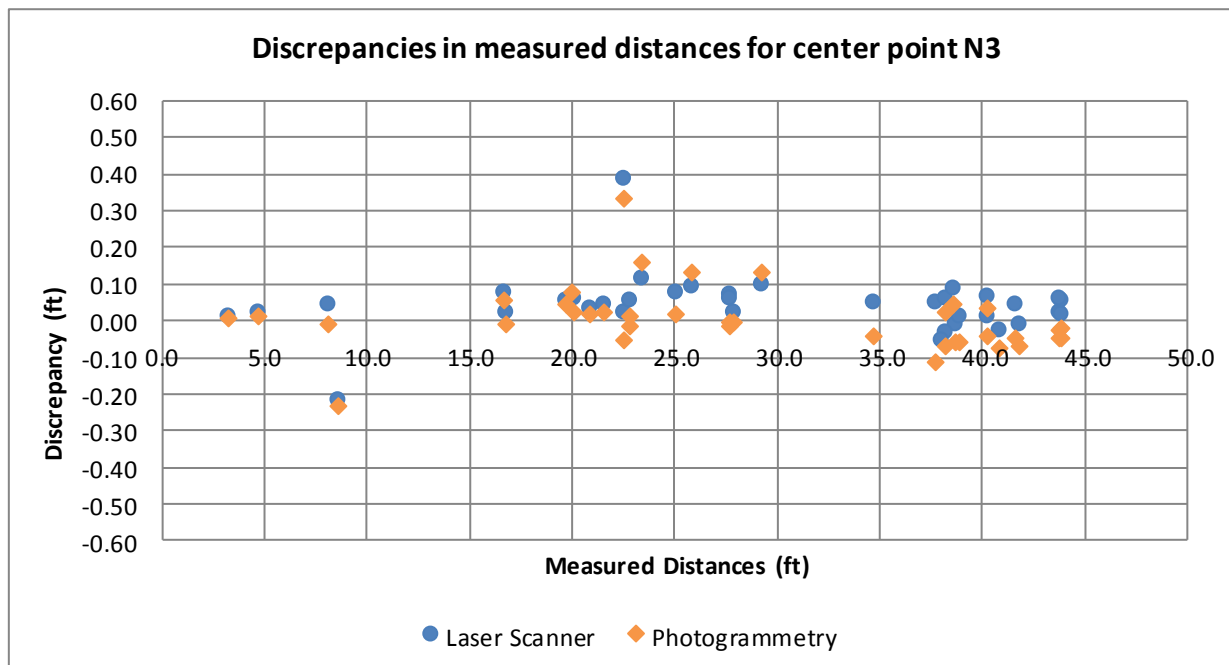


Figure 12: Discrepancies in Measured Distances from Center Point N3, at Mayan Temple

Item	Laser Scanner - Total Station	Photogrammetry - Total Station
Maximum Value (ft)	0.2178	0.2350
Minimum Value (ft)	0.0084	0.0026
Mean Value (ft)	0.0522	0.0534
RMS Value (ft)	0.0641	0.0694
Standard Deviation (ft)	0.0391	0.0492
Outliers Removed	N7, W2	S7, W2

Table 7: Statistical Data of Distance Discrepancies Measured from Center Point N3, with Outliers Removed, at Mayan Temple

Item	Laser Scanner - Total Station	Photogrammetry - Total Station
Maximum Value (ft)	0.0968	0.0987
Minimum Value (ft)	0.0008	0.0006
Mean Value (ft)	0.0411	0.0378
RMS Value (ft)	0.0509	0.0456
Standard Deviation (ft)	0.0316	0.0279
Outliers Removed	N7, S1	E9, S1

Table 8: Statistical Data of Distance Discrepancies Measured from Center Point S5, with Outliers Removed, at Mayan Temple

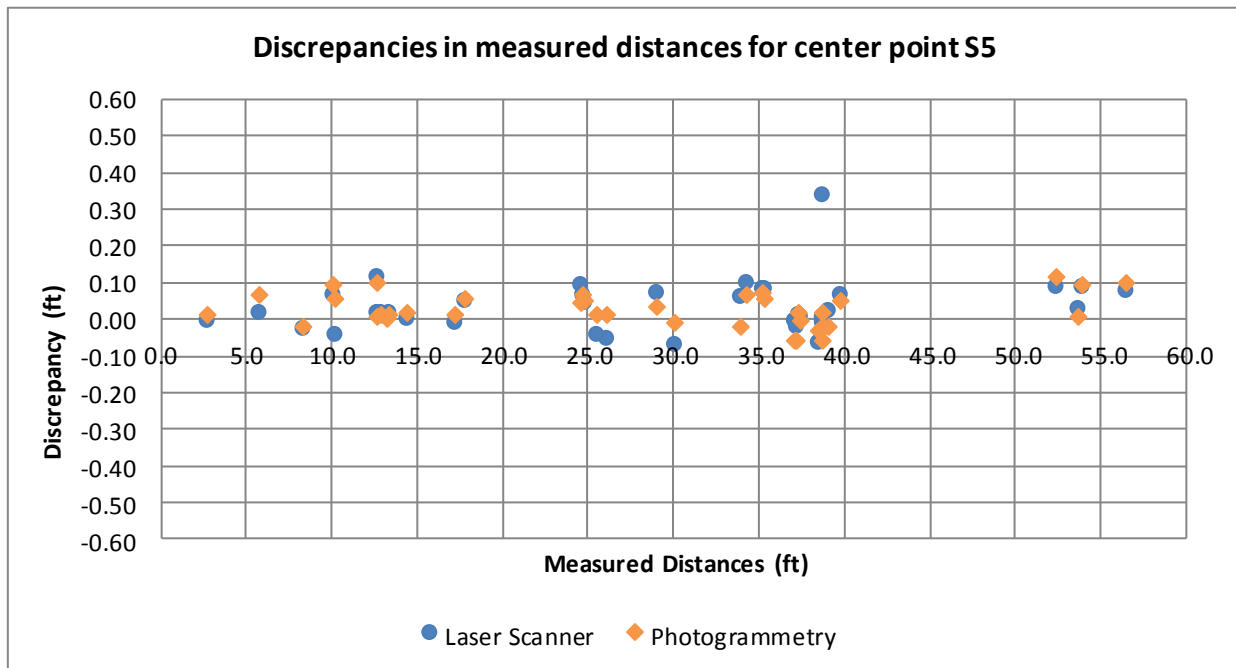


Figure 13: Discrepancies in Measured Distances from Center Point S5, at Mayan Temple

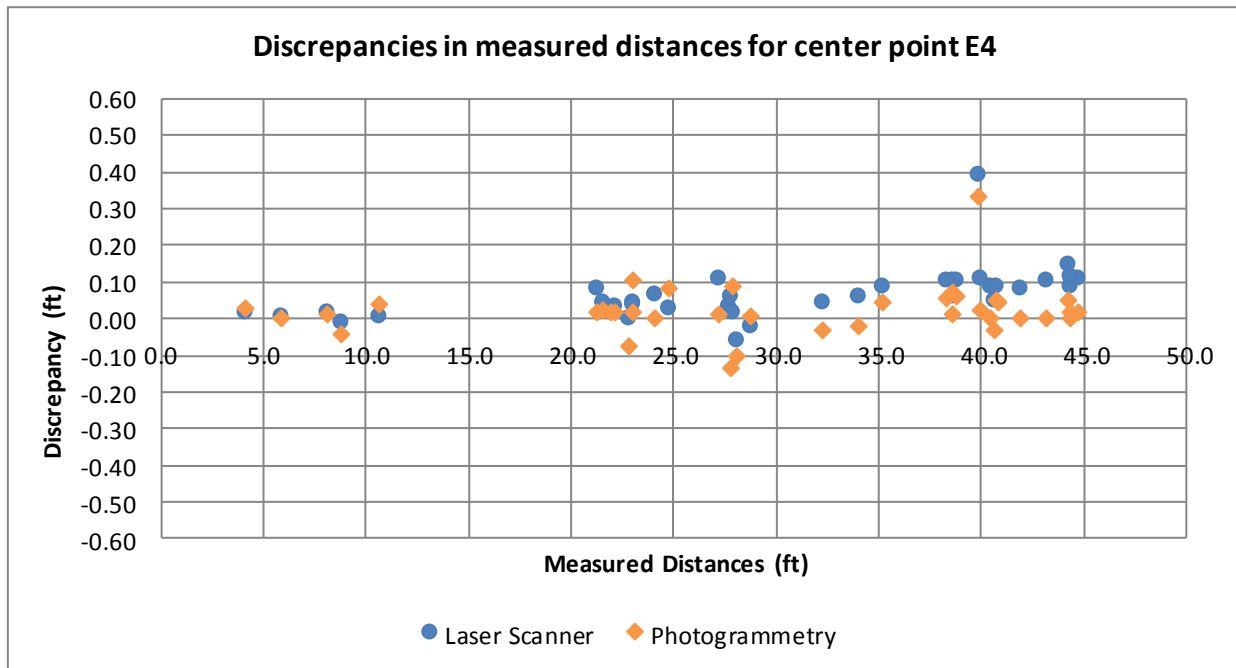


Figure 14: Discrepancies in Measured Distances from Center Point E4, at Mayan Center

Item	Laser Scanner - Total	Photogrammetry - Total
Maximum Value (ft)	0.1490	0.1340
Minimum Value (ft)	0.0001	0.0000
Mean Value (ft)	0.0614	0.0375
RMS Value (ft)	0.0714	0.0485
Standard Deviation (ft)	0.0388	0.0335
Outliers Removed	N7, W2	S7, W2

Table 9: Statistical Data of Distance Discrepancies Measured from Center Point E4, with Outliers Removed, at Mayan Temple

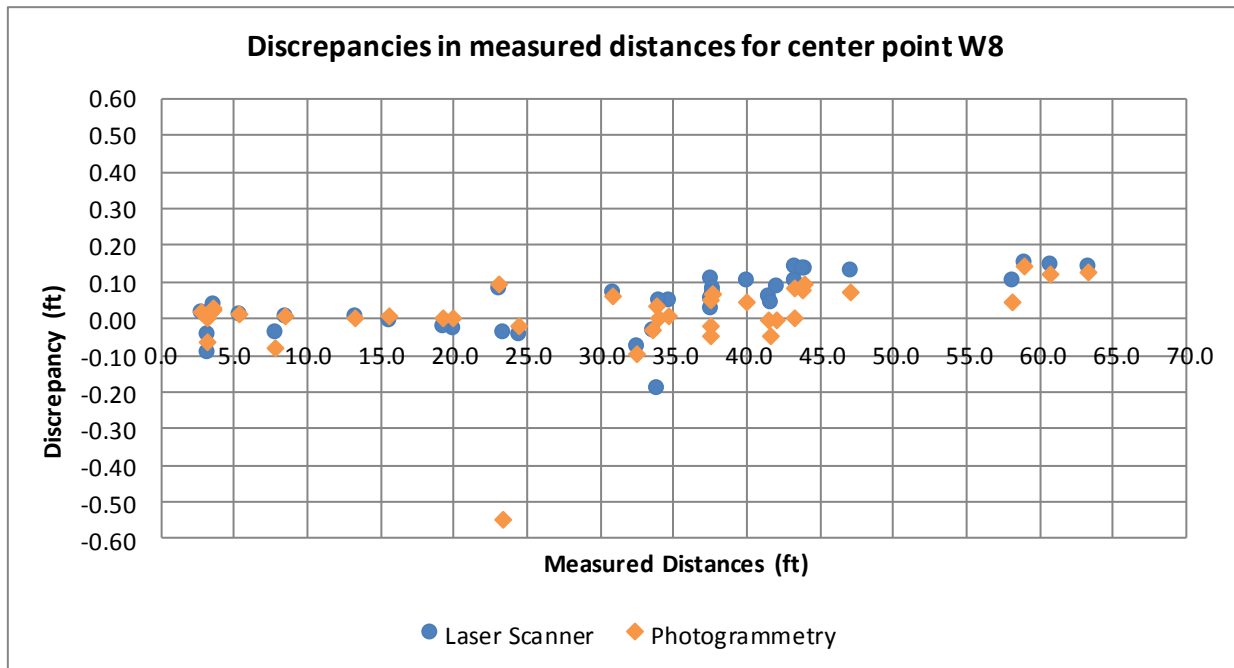


Figure 15: Discrepancies in Measured Distances from Center point W8, at Mayan Temple

Item	Laser Scanner - Total Station	Photogrammetry - Total Station
Maximum Value (ft)	0.1478	0.1251
Minimum Value (ft)	0.0044	0.0000
Mean Value (ft)	0.0667	0.0441
RMS Value (ft)	0.0786	0.0547
Standard Deviation (ft)	0.0441	0.0368
Outliers Removed	N7, E9	S7, E9

Table 10: Statistical Data of Distance Discrepancies Measured from Center Point W8, with Outliers Removed, at Mayan Temple

5 OBSERVATIONS AND RECOMMENDATIONS

The two cases considered in this study present similar discrepancies in distances measured within the resulting 3D virtual models versus the same distances measured, in the field, with a classical total-station instrument. Two different virtual models were considered for each structure, one based on close-range photogrammetry and other based on laser-scanned point

clouds. Case 1 consisted of a relatively small, one-story, storage building, where distance measurements ranged, approximately, from 2 ft to 20 ft (\approx from 0.6 m to 6.1 m). Case 2 involved a larger three-level structure, where distance measurements ranged approximately, from 5 ft to 60 ft (\approx from 1.5 m to 18.3 m). As observed in Table 11, in Case 1, Storage Building, the averaged mean discrepancy of measurements within the 3D laser-based model and the total-station instrument was 0.031 ft. Similarly, the averaged mean discrepancies between the photogrammetric measurements and those obtained with the total-station instrument was 0.042 ft. Regarding the averaged standard deviations of those discrepancies, they were 0.056 ft and 0.057 ft, respectively.

Overall Results (feet) for Case1, Storage Building				
Central Points	Overall Discrepancies in Measured Distances from Central Points			
	Mean Values		Standard Deviations	
	Scan - Tot Sta.	Photogr. -Tot Sta.	Scan - Tot Sta.	Photogr. -Tot Sta.
A066	0.039	0.046	0.067	0.056
B013	0.012	0.023	0.017	0.019
C035	0.019	0.039	0.024	0.030
D022	0.052	0.061	0.122	0.121
Overall Averages	Averaged Mean Values		Averaged Standard Deviations	
	0.031	0.042	0.057	0.056
	Average of both Approaches		Average of both Approaches	
	0.036		0.057	

Table 11: Overall Results for Storage Building with Distances Ranging from 2 ft to 20 ft

As shown in Table 12 for Case 2, Mayan Temple, the averaged mean discrepancy of measurements within the 3D laser-based model and the total-station instrument was 0.055 ft. Similarly, the averaged mean discrepancies between the photogrammetric measurements and those obtained with the total-station instrument was 0.043 ft. Regarding the averaged standard deviations of those discrepancies, they were 0.038 ft and 0.037 ft, respectively. Given these similar magnitudes, it is observed that, for this range of measurements, the CRP models could be employed as an alternative measuring tool.

Overall Results (feet) for Case 2, Mayan Temple				
Central Points	Overall Discrepancies in Measured Distances from Central Points			
	Mean Values		Standard Deviations	
	Scan - Tot Sta.	Photogr. -Tot Sta.	Scan - Tot Sta.	Photogr. -Tot Sta.
N3	0.052	0.053	0.039	0.049
S5	0.041	0.038	0.032	0.028
E4	0.061	0.038	0.039	0.034
W8	0.067	0.044	0.044	0.037
Overall Averages	Averaged Mean Values		Averaged Standard Deviations	
	0.055	0.043	0.038	0.037
	Average of both Approaches		Average of both Approaches	
	0.049		0.038	

Table 12: Overall Results for Mayan Temple with Distances Ranging from 5 ft to 60 ft

The photogrammetry models required high-resolution, clear pictures. The resolution of the employed cameras play an important part in the end result. The highest megapixel camera within budget should be used, especially if equipped with a fixed wide angle lens. It is well-known that as the distance from the object to the lens increases, it causes loss of detail in the picture and in the completed model. It was observed that the wide angle lens would lose detail when it was more than 100 ft. away from the object being photographed. This type of lens should be used as close to the object as possible while still keeping a good field of view. Another observation indicated that models tend to fail processing when less than sixty percent overlap is used between photos and when the photos are not taken perpendicular to the object. It is recommended by PhotoScan to set the camera to save the pictures in RAW format and then convert them to lossless TIFF format using another program. Additionally, the photogrammetry model will usually require the use of drones if the structure is over one story or if topography is being captured. Another consideration is how many pictures will be necessary to complete a project. The computer used in this study can process 100 to 200 pictures into a model in about an hour. When the photo set grows to over 500 pictures, it may require that computer a week or more than a month to generate the model. The processing time can be reduced by employing workstation or server class computers. Workstations and servers have the option to have numerous multiple processors and over 128 gigabytes of memory, which will significantly reduce the use of the hard drive swap file. The picture limitations observed in this study suggest that photogrammetry tends to be viable when producing low detail large projects such as terrain mapping or high detail small projects such as the ones presented in this study.

The main observation made when using laser scanners and CRP is that scanners require more time to capture data and less time to post-process it. The currently available long-range scanners are powerful and accurate instruments. It is also well-known how the distance to the object affects the scanned model. Certainly, as objects are farther away from the scanner, the acquired point density decreases. This would increase the difficulty of selecting accurate points to make measurements and, in turn, it affects the accuracy of the measurements being made. A good recommendation is to keep the laser scanner as close to the object as possible or increase the number of scans when this is not possible. The resolution can also be increased, but that will increase the amount of time per scan. Another option is to scan important sections using a windowed scan with maximum resolution. The type of scanning targets selected influences the overall registration error. The targets used in this study with the highest accuracy were the spheres because they do not need to be readjusted to face the scanner after moving to a new scanning station. Another observation is to complete the scanning in one day if possible. Each time targets are repositioned, it introduces additional error into the registration as there is always some repositioning inaccuracies. Additionally, if the project requires the scanning of blue or black sections expect to increase the resolution or decrease the scanner-to-object distance. This is due to the fact that blue and black colors have very low reflectance of light.

ACKNOWLEDGEMENTS

The authors express their sincere gratitude to Professor Carlos Wabi Peniche and all involved personnel from Universidad Anáhuac Mayab and the Mexican National Institute of Anthropology and History for assisting and allowing a group of 14 members (students and faculty) from Georgia Southern University to access and measure the Temple of the Seven Dolls at Dzibilchaltun during four weeks in the summer 2015.

Additionally, the corresponding author is strongly grateful for having been invited to participate in a symposium at ENIEF 2016 to honor his former Argentinean professor, Dr. Luis A. Godoy, an outstanding civil engineer, educator and researcher who 35 years ago served as his mentor and soon became his role model.

REFERENCES

- Dai, F., Rashidi, A., Brilakis, I. and Vela, P., Comparison of Image-Based and Time-of-Flight-Based Technologies for Three-Dimensional Reconstruction of Infrastructure. *Journal of Construction Engineering and Management*, 139(1):69-79, 2013.
- Dai, F. and Lu, M., Assessing the Accuracy of Applying Photogrammetry to Take Geometric Measurements on Building Products. *Journal of Construction Engineering and Management*, 2013.
- Ghosh, S.K., *Fundamentals of Computational Photogrammetry*. New Delhi: Concept Publishing Company, 2005.
- Grussenmeyer, P., Landes, T., Voegtle, T. and K Ringle, K. Comparison Methods of Terrestrial Laser Scanning, Photogrammetry, and Techeometry Data for Recording of Cultural Heritage Buildings. *The International Archives of the Photogrammetry, Remote Sensing and Spatial Information Sciences*, 37(B5):213-218, 2008.
- Matthews, N.A., *Aerial and Close-Range Photogrammetric Technology: Providing Resource Documentation, Interpretation, and Preservation*. Technical Note 428, Denver: U.S. Department of the Interior, Bureau of Land Management, 2008.
- Sužiedelytė-Visockienė, J., Bagdžiūnaitė, R., Malys, N. and Maliene, V., Close-Range Photogrammetry Enables Documentation of Environment-Induced Deformation of Architectural Heritage. *Environmental Engineering and Management Journal*, 14(6):1371-1381, 2015.
- Yakar, M., Yilmaz, H.M., and Mutluoglu, O., Close Range Photogrammetry and Robotic Total Station in Volume Calculation. *International Journal of the Physical Sciences* 5(2):86-96, 2010.